

Rendezvous & Proximity Operations

ME 601 (Autonomous Feedback) Final Project

Ian Ruh

University of Wisconsin - Madison

Abstract—Using the material covered in class, this project analyzes the control and relative dynamics of two spacecraft in orbit around earth by designing, implementing, and testing several linear-quadratic-regulator (LQR) and **model predictive control (MPC)** controllers. This is a subject of interest due to its current usage in vehicle docking to space stations, as well as its future applications to in-orbit debris collection, in-orbit assembly, and in-orbit refueling.

We designed and implemented three infinite LQR feedback controllers: an infinite LQR controller using the linearized system dynamics that just stabilizes the system at the origin; a trajectory tracking infinite LQR controller using the linearized system's error dynamics; and a time varying infinite LQR feedback controller that uses a nonlinear, but simplified, version of the system's error dynamics. We also designed and implemented an MPC controller using the linearized system dynamics, while incorporating state and control constraints.

To test our controllers, we wrote a restricted two-body simulator to simulate the dynamics of both the target and chaser vehicles. For simplicity, we modeled the Earth as a perfect sphere and only considered the idealised dynamics due to gravity.

In order to further simplify the problem, several assumptions on the orbital parameters of the two spacecrafts, the configuration of actuators, the ideal behavior of the actuators, the control of the spacecraft attitude and knowledge of the spacecraft state will be made. These assumptions and their impact are discussed in the next section.

I. INTRODUCTION

The rendezvous of two space craft, or more generally the relative positioning of two spacecraft in orbit, is a complex problem due to the dynamics involved. The first step in approaching the problem is to select a coordinate system in which the relative dynamics will be studied.

A. Coordinate Systems

In the rest of this document, we identify two spacecrafts: the target and the chaser (also referred to as the chief and follower). The target is assumed to have attitude control such that it maintains a consistent orientation with respect to earth's horizon, but is otherwise inert. The chaser is the vehicle that we focus on controlling the position of.

The Earth Centered Inertial (ECI) frame [2] is used as our reference inertial frame and is used for numerical propagation of the system dynamics. As Earth orbits the sun, the ECI frame remains in the same orientation relative to the stars. Similarly, as Earth rotates around its axis, the ECI frame remains fixed relative to the stars.

In the context of rendezvous and proximity operations, it is convenient to identify the the Radial-Transverse-Normal

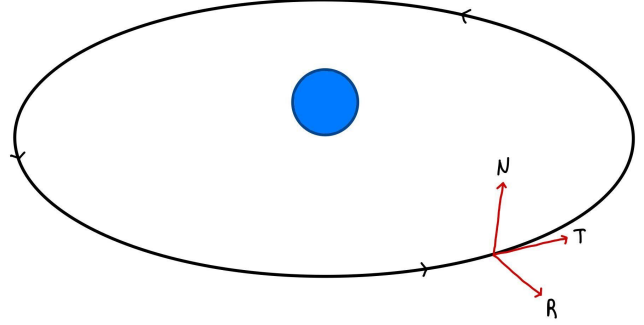


Fig. 1. Radial-Transverse-Normal (RTN) Coordinate Frame

(RTN) coordinate frame centered with the origin at the center of mass of the target vehicle, as shown in figure 1. The three axes are aligned in the radial direction, along the vector from the origin of the center of the earth; the transverse direction, parallel to the velocity vector, and thus along the orbital path; and the normal direction, parallel to the orbit's angular momentum vector.

Analyzing the chaser's dynamics and control in the RTN frame has the advantage of much smaller oscillations in the position-velocity coordinates as well as conveniently placing out target state at the origin.

Notice that as the target orbits the central body, the RTN frame rotates relative to the inertial frame of the central body, so the relative position and dynamics of the chaser is not just a translation from the inertial frame.

We also define our position-velocity (PV) state vector within both the ECI frame and the RTN frame as $[\vec{x}|\vec{v}]^T = [x, y, z, v_x, v_y, v_z]^T$ with respect to each frame. Though not the state representation primarily used in this project, several of the states from the classical orbital elements (COE) are of import. The full COE state vector is

$$\begin{aligned} e &= \text{Eccentricity} \\ a &= \text{Semi-major axis (SMA)} \\ i &= \text{Inclination} \\ \omega &= \text{Argument of perigee} \\ \Omega &= \text{Right ascension of the ascending node (RAAN)} \\ f &= \text{True anomaly} \end{aligned} \tag{1}$$

For this project, the three important states are: the eccentricity, which is the eccentricity of our orbit's ellipse; SMA,

which (for our purposes) describes the orbital radius; and the true anomaly, which describes, unlike the other states, where within the orbit we are, rather than the shape or orientation of the orbit.

B. Relative Dynamics

Within the RTN coordinate frame the following relative dynamics can be derived [6]:

$$\begin{aligned}\ddot{x} - 2\dot{f}_c\dot{y} - \ddot{f}_cy - \dot{f}_c^2x &= \frac{-\mu(r_c + x)}{[(r_c + x)^2 + y^2 + z^2]^{3/2}} + \frac{\mu}{r_c^2} + d_R \\ \ddot{y} + 2\dot{f}_c\dot{x} + \ddot{f}_cx - \dot{f}_c^2y &= \frac{-\mu y}{[(r_c + x)^2 + y^2 + z^2]^{3/2}} + d_T \\ \ddot{z} &= \frac{-\mu z}{[(r_c + x)^2 + y^2 + z^2]^{3/2}} + d_N\end{aligned}\quad (2)$$

Where f_c is the target's true anomaly, r_c is the target's radius, and $\vec{d} = [d_R, d_T, d_N]^T$ represents the relative disturbing accelerations between the target and the chaser in the target's RTN frame.

The first simplifying assumption we make is on the eccentricity of the target's orbit. If the target's orbit is near circular (the eccentricity is near 0), then $\dot{f}_c = \text{mean motion} = \sqrt{\frac{\mu}{a^3}}$, where μ is the earth's gravitational parameter ($\approx 3.986 \cdot 10^{14} \text{ m}^2/\text{s}$), and a is the orbit's semi-major axis (SMA). Thus, \dot{f}_c is constant and $\ddot{f}_c = 0$. In addition, the target's radius is constant and $r_c = a_c$, where a_c is the target's SMA. This leads to the following simplified dynamics:

$$\begin{aligned}\ddot{x} &= -\frac{\mu(r_c + x)}{[(r_c + x)^2 + y^2 + z^2]^{3/2}} + \frac{\mu}{r_c^2} + 2n\dot{y} + n^2x + d_R \\ \ddot{y} &= -\frac{\mu y}{[(r_c + x)^2 + y^2 + z^2]^{3/2}} + 2n\dot{x} + n^2y + d_T \\ \ddot{z} &= -\frac{\mu z}{[(r_c + x)^2 + y^2 + z^2]^{3/2}} + d_N\end{aligned}\quad (3)$$

Linearizing this around the target's position, we arrive at the following linear dynamics known as the Hill-Clohessy-Wiltshire equations [5]:

$$\begin{aligned}\ddot{x} &= 3n^2x + 2n\dot{y} + d_R \\ \ddot{y} &= -2n\dot{x} + d_T \\ \ddot{z} &= -n^2z + d_N\end{aligned}\quad (4)$$

Which we can express in the standard state space form

$$\begin{aligned}\dot{x}_0 &= x_3 \\ \dot{x}_1 &= x_4 \\ \dot{x}_2 &= x_5 \\ \dot{x}_3 &= 3n^2x_0 + 2nx_4 + d_R \\ \dot{x}_4 &= -2nx_3 + d_T \\ \dot{x}_5 &= -n^2x_2 + d_N\end{aligned}\quad (5)$$

C. Other Assumptions

The reality of controlling a spacecraft involves complex actuators, possibly including electric propulsion, mono-propellant attitude control systems, reaction wheels, control moment gyros, magnetic torquers, and others that all of their own dynamics and constraints (such as burn times, thrust profiles, discrete or continuous thrust levels, etc) that need to be accounted for in practice. For the purposes of this project, only the dynamics due to gravity and accelerations in the RTN frame are considered to simplify the analysis. Therefore, we are neglecting the attitude control of the chaser and the arrangement (and therefore selection of thrusters) such that we have a force in the RTN frame as our only control input. However in reality, there may be significant efficiency gains that can be realized by considering the arrangement of thrusters when planning maneuvers.

In addition to assumptions on the actuators, we also assume that we have perfect knowledge of both the target's and chaser's state vector. However, state estimation for spacecraft is a significant challenge, and, depending on the location (e.g. close enough for relative positioning systems), the uncertainty in our knowledge can be quite significant.

II. SIMULATION

In order to test the controllers implemented, we created a simulation environment and several test scenarios to evaluate their performance [3]. The source code is available at <https://github.com/ianruh/Rendezvous-Proximity>.

We wrote a restricted two body simulator to propagate the target and chaser in the ECI frame around Earth. All nonidealities of the orbits, including oblateness perturbations, solar radiation pressure, lunar perturbations, etc., were neglected. Due to the relatively small timescales, distances, and parameters of the scenarios, these effects would be small, though should not be ignored in practice.

At every control time step, the chaser's state vector was converted into a PV vector in the RTN coordinate frame relative to the target. The simulator saturated the control at 0.01 m/s/s, which is reasonable for the monoprop thrusters on a relatively small satellite.

The controllers for tracking trajectories were provided a target state at each control time step, where the target state was generated analytically or read (and interpolated) from a CSV file depending on the scenario.

III. CONTROLLERS

A. Infinite LQR Linear Controller

Using the Hill-Clohessy-Wiltshire (4) expressed as matrices in state space form, we implemented an infinite LQR controller that solves the following problem:

$$\begin{aligned}\min_{x,u} \quad & \frac{1}{2} \int_{t_0}^{\infty} (x(t)^T \mathbf{Q}x(t) + u(t)^T \mathbf{R}u(t)) dt \\ \text{s.t.} \quad & \dot{x} = \mathbf{A}x + \mathbf{B}u \\ & x(t_0) = x_0\end{aligned}\quad (6)$$

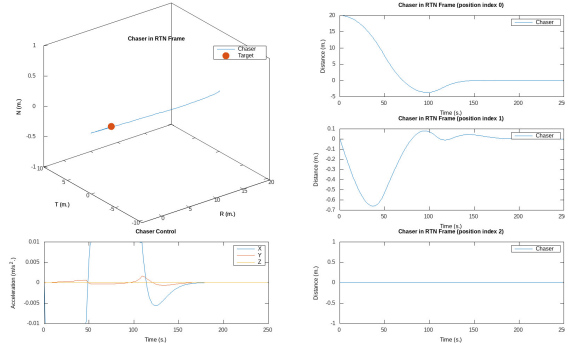


Fig. 2. Orbit stabilization starting from 20 meter larger radius.

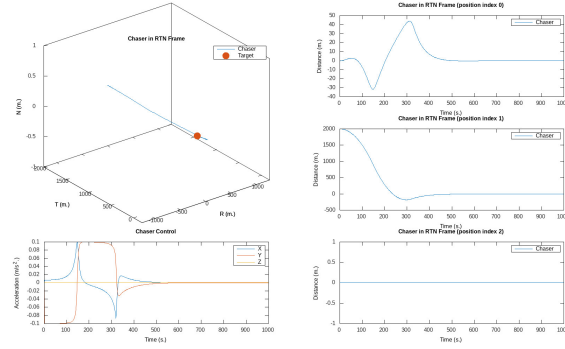


Fig. 3. Orbit stabilization starting from 2000 meters ahead.

Where \mathbf{A} and \mathbf{B} are defined as

$$\mathbf{A} = \begin{bmatrix} 0 & 0 & 0 & 1 & 0 & 0 \\ 0 & 0 & 0 & 0 & 1 & 0 \\ 0 & 0 & 0 & 0 & 0 & 1 \\ 3n^2 & 0 & 0 & 0 & 2n & 0 \\ 0 & 0 & 0 & -2n & 0 & 0 \\ 0 & 0 & -n^2 & 0 & 0 & 0 \end{bmatrix} \quad (7)$$

$$\mathbf{B} = \begin{bmatrix} 0 & 0 & 0 \\ 0 & 0 & 0 \\ 0 & 0 & 0 \\ 1 & 0 & 0 \\ 0 & 1 & 0 \\ 0 & 0 & 1 \end{bmatrix}$$

and $\mathbf{Q} = I_{6 \times 6}$, $\mathbf{R} = I_{3 \times 3}$. This controller stabilizes the chaser in the vicinity of the target. Two scenarios are shown in figures 2 and 3.

Q and R weight matrices

The linear infinite LQR control is able to stabilize the chaser around the target, though the size of this region of stability appears to be significantly dependent on the weight matrices \mathbf{Q} and \mathbf{R} chosen.

These weights were selected by trial and error, but the starting point was chosen based on the heuristic of weighting

$$\frac{1}{(\text{error bound})^2} \cdot$$

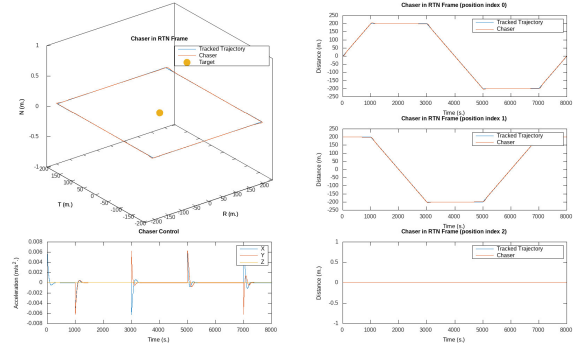


Fig. 4. Box trajectory tracking at GEO altitude (≈ 35000 km).

Aside from showing that our dynamics and basic approach work, these controllers would have little practical use for rendezvous and docking, where safety constraints on the spacecraft state (both position and velocity) are very important. Therefore, we also implemented and tested two trajectory tracking controllers, as discussed in the next section.

B. Infinite LQR Time Invariant Trajectory Tracking Controller

We implemented an LQR trajectory tracking controller based on the error dynamics of the linearized system in (4). We define the state error $e(t) = x(t) - x_d(t)$, where x_d is our desired trajectory, and the control error $v(t) = u(t) - u_d(t)$, where u_d is our desired control. Then the error dynamics are

$$\begin{aligned} \dot{e} &= \dot{x} - \dot{x}_d \\ &= f(x, u) - f(x_d, u_d) \\ &= f(x_d + e, u_d + v) - f(x_d, u_d) \\ &= (\mathbf{A}(x_d + e) + \mathbf{B}(u_d + v)) - (\mathbf{A}x_d + \mathbf{B}u_d) \\ &= \mathbf{A}e + \mathbf{B}v \end{aligned} \quad (8)$$

Where \mathbf{A} and \mathbf{B} are the same as in (7). Conveniently, the error dynamics of the linearized system are identical to the dynamics of the linearized system.

Being provided a trajectory to track, one which can be guaranteed not to violate any safety constraints, is a more realistic scenario than just an LQR controller attempting to stabilize the system at the origin.

We tested the trajectory tracking controllers on several 'box' trajectories at varying orbital radii from Geo Synchronous (42,000 km) to LEO (8,000 km).

As the orbit got smaller, the disturbing acceleration required to cancel out the dynamics of the system begins to saturate the inputs, causing a loss of control. This behavior is expected, as the 'box' trajectories ignore the natural dynamics of the system, which become more significant the smaller the orbit gets.

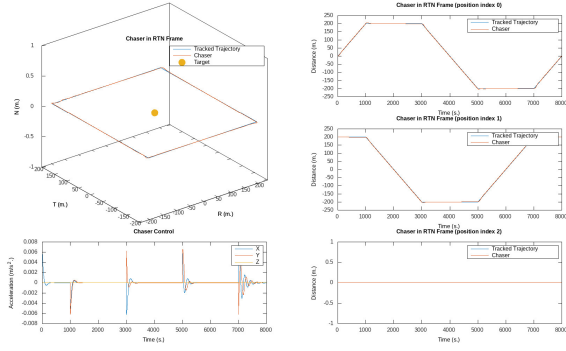


Fig. 5. Box trajectory tracking at 30000 km SMA.

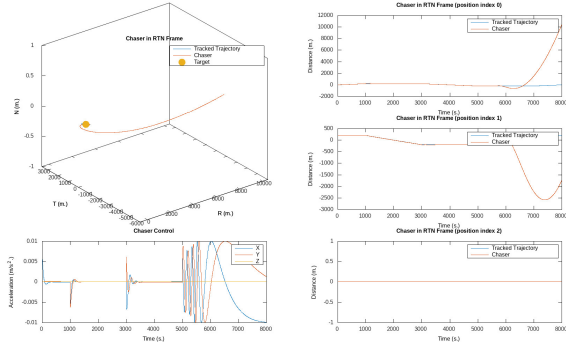


Fig. 6. Box trajectory tracking at 20000 km SMA.

C. Infinite LQR Time Varying Trajectory Tracking Controller

We implemented an LQR trajectory tracking controller based off of the nonlinear dynamics shown in eq. 3.

$$\begin{aligned}
 \dot{e} &= \dot{x} - \dot{x}_d \\
 &= f(x, u) - f(x_d, u_d) \\
 &= f(x_d + e, u_d + v) - f(x_d, u_d) \\
 &= F(e, v, x_d(t), u_d(t))
 \end{aligned} \tag{9}$$

The time varying linearized error dynamics are then given by

$$\dot{e} = \mathbf{A}(t)e + \mathbf{B}(t)v \tag{10}$$

where

$$\mathbf{A}(t) = \frac{\partial F}{\partial e} \bigg|_{x_d(t), u_d(t)} \tag{11}$$

$$\mathbf{B}(t) = \frac{\partial F}{\partial v} \bigg|_{x_d(t), u_d(t)} \tag{12}$$

Rather than performing the derivation by hand, we used the symbolic mathematics library SymEngine [4] to derive the symbolic matrices for $\mathbf{A}(t)$ and $\mathbf{B}(t)$. From the symbolic matrices, we performed code generation at runtime to create a function for each symbolic matrix that, given a vector of the

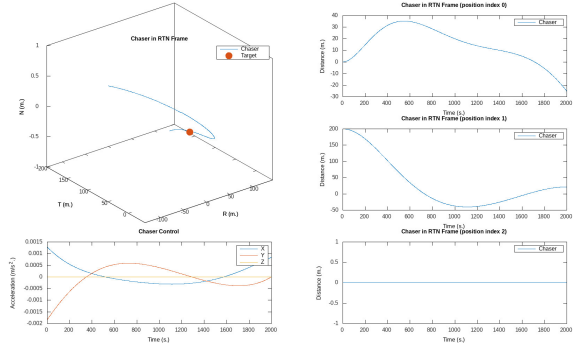


Fig. 7. MPC controller bringing the chaser to the target when starting 200M away.

desired state and control, returned \mathbf{A} and \mathbf{B} . The generated code was compiled to a shared object and then loaded into memory and the function pointers retrieved.

D. MPC Controller

We implemented a discrete time MPC controller based off of Hill-Clohessey-Wiltshire equations (4), which constrained the maximum control, velocity, and state. The MPC controller was implemented using [1], and formulated as:

This

$$\begin{aligned}
 \min_{x, u} \quad & \frac{1}{2} \int_{t_0}^{\infty} (x(t)^T \mathbf{Q} x(t) + u(t)^T \mathbf{R} u(t)) dt \\
 \text{s.t.} \quad & \dot{x} = \mathbf{A}x + \mathbf{B}u \\
 & x(t_0) = x_0
 \end{aligned} \tag{13}$$

As this was not formulated as a tracking controller (though it could be easily adapted to one by parameterizing goal state in the objective for every timestep), we tested this controller on just bringing the chaser to the target when started within the vicinity of the target.

IV. EXTENSIONS

There are many extensions and variations on the system and the controllers that could be explored. Of interest to myself is extending the LTV controller to the noncircular case, where the first and second time derivatives of the true anomaly come into the system. This would enable the controllers to function in a larger vicinity of the target, as well in elliptical orbits.

Similarly, it would be interesting to extend the simulation and controllers to the restricted three body problem involving the earth, moon, and spacecraft. Of particular interest, would be rendezvous and proximity operations in Near Rectilinear Halo Orbits about the Moon (these are extremely elliptical lunar orbits that verge on being closer to L2 halo orbits than lunar orbits) where the planned NASA Gateway manned space station will be.

The assumptions made about the configuration and actuators could also be removed, specifically the arrangement of thrusters and it's impact the efficiency of maneuvers would be interesting.

REFERENCES

- [1] Cppmpc github repo. <https://github.com/ianruh/cppmpc>.
- [2] Earth-cetered inertial frame. https://en.wikipedia.org/wiki/Earth-centered_inertial.
- [3] Rendezvous-proximity github repo. <https://github.com/ianruh/Rendezvous-Proximity>.
- [4] Symengine. <https://github.com/symengine/symengine>.
- [5] Eugene M Cliff. Clohessy - Wiltshire Analysis. *N/A*, page 4, *N/A*.
- [6] Joshua Sullivan, Sebastian Grimberg, and Simone D'Amico. Comprehensive Survey and Assessment of Spacecraft Relative Motion Dynamics Models. *Journal of Guidance, Control, and Dynamics*, 40(8):1837–1859, August 2017.